

**\*\*FULL TITLE\*\***

*ASP Conference Series, Vol. \*\*VOLUME\*\*, \*\*YEAR OF PUBLICATION\*\**

**\*\*NAMES OF EDITORS\*\***

## **Microlensing Searches for Planets: Results and Future Prospects**

B. Scott Gaudi

*Department of Astronomy, The Ohio State University, 140 W. 18th Ave., Columbus, OH 43210*

**Abstract.** Microlensing is potentially sensitive to multiple-planet systems containing analogs of all the solar system planets except Mercury, as well as to free floating planets. I review the landscape of microlensing planet searches, beginning with an outline of the method itself, and continuing with an overview of the results that have been obtained to date. Four planets have been detected with microlensing. I discuss what these detections have taught us about the frequency of terrestrial and giant planets with separations beyond the “snow line.” I then discuss the near and long-term prospects for microlensing planet searches, and in particular speculate on the expected returns of next-generation microlensing experiments both from the ground and from space. When combined with the results from other complementary surveys, next generation microlensing surveys can yield an accurate and complete census of the frequency and properties of essentially all planets with masses greater than that of Mars.

### **1. Introduction**

*“I don’t understand. You’re looking for planets you can’t see around stars you can’t see.”* – Debra Fischer, c. 2000

*“Microlensing is a cult.”* – Dave Koerner, c. 2000

At the time when these words were uttered, microlensing planet searches had not yet made any definitive detections, despite having been in production in earnest for over five years, and despite the fact that numerous talks had been given vociferously extolling the virtues of the method. Furthermore, it was a well-known ‘fact’ (in part perpetuated by those giving said talks [including myself]) that the primary virtue of the microlensing method was its ability to provide statistics on large-separation and low-mass planets. Individual detections would be of little interest, it was thought, because there would be no opportunity for follow-up and the properties of the host stars would remain unknown, due primarily to their very large distances from Earth.

It is now seven years later, and the landscape and perception of microlensing planet searches has changed dramatically. Four detections have been published, and an additional  $\sim$ half a dozen planets have been detected and will be announced in the not-to-distant future. The four published detections have already provided new and important information about the frequency of “Super Earths” and Jovian planets with separations beyond the “snow line.” Furthermore, it has become clear that the original assessments of the (im)possibility of follow-up

and characterization of the planet host stars were overly pessimistic. Indeed, for three of the four detected planets, reasonably precise ( $\sim 20\%$ ) estimates of the mass of the host star have been made or will soon be possible.

## 2. How Microlensing Finds Planets

A microlensing event occurs when a foreground “lens” happens to pass very close to our line of sight to a more distant background “source.” For our purposes, the lens is a main-sequence star or stellar remnant in the foreground Galactic disk or bulge, whereas the source is a main-sequence star or giant typically in the bulge. If the lens is exactly aligned with the source, it images the source into an “Einstein ring” with a radius  $\theta_E = \sqrt{\kappa M \pi_{\text{rel}}}$ , where  $M$  is the mass of the lens,  $\pi_{\text{rel}} = \text{AU}/(d_l^{-1} - d_s^{-1})$  is the lens-source relative parallax,  $d_l$  and  $d_s$  are the distances to the source and lens, and  $\kappa = 4G/c^2 \text{AU}$ . In the case of imperfect alignment, the lens creates two images of the source which have splittings near the time of closest alignment of  $\sim 2\theta_E$ . For typical lens masses ( $0.1 - 1 M_\odot$ ) and lens and source distances ( $1 - 10 \text{ kpc}$ ),  $\theta_E \sim 500 \mu\text{as}$  and so the images are not resolved. However, the images are also magnified, by an amount  $A$  that depends only on  $u \equiv \theta/\theta_E$ , the angular separation of the lens and source  $\theta$  in units of  $\theta_E$ . For  $u \ll 1$ , the magnification takes on the simple form  $A \simeq 1/u$ .

The transverse motion of the lens, source, and observer results in a time-variable magnification and gives rise to a smooth, symmetric microlensing event with a characteristic form. The magnification is  $A > 1.34$  for  $u \leq 1$ , and so the magnifications are substantial and easily detectable. Typically, observations of a microlensing event caused by an isolated lens can fit by a simple four parameter model. Three specify the magnification as a function of time: the minimum angular separation  $u_0$  of the lens and source in units of  $\theta_E$  (the impact parameter, which also specifies the maximum magnification), the time of maximum magnification, and finally the Einstein timescale,  $t_E \equiv \theta_E/\mu$ , where  $\mu$  is the relative lens-source proper motion. The typical timescales for events toward the Galactic bulge are of order a month. Only  $t_E$  contains any information about the physical properties of the lens, and then only in a degenerate combination of the lens mass, distance, and transverse velocity. However, as mentioned below, it has proven to be the case that it is often possible to obtain additional information which partially or totally breaks this degeneracy. The remaining two parameters required to fit a single-lens event are the flux of the source, and the flux of any unresolved light that is not being lensed. The latter can include light from a companion to the source, light from unrelated nearby stars, light from a companion to the lens, and (most interestingly) light from the lens itself. In those cases where it is possible to isolate the light from the lens itself, this measurement can be used to constrain the lens mass (Bennett et al. 2007a).

If the lens star happens to have a planetary companion, the companion can create a short-timescale perturbation on the primary microlensing event (Mao & Paczynski 1991; Gould & Loeb 1992). There are two conceptually different channels by which planets can be detected with microlensing.

In the main channel, the planet happens to be located near the path of one of the two images created by primary lens. As the image sweeps by the position of the planet, the planet will further perturb the light from this image

and yield a short-timescale deviation (Gould & Loeb 1992). The duration of this deviation is  $t_p \sim q^{1/2} t_E$ , where  $q = m_p/M$  is the mass ratio and  $m_p$  is the planet mass. Thus the duration of the perturbation ranges from a few hours for an Earth-mass planet to a day for Jovian-mass planets. The location of the perturbation relative to the peak of the primary event depends on the angle of the projected star-planet axis, as well as the instantaneous angular separation between the planet and host star in units of  $\theta_E$ . Since the orientation of the source trajectory relative to the planet position is random, the time of this perturbation is not predictable and the probability is  $\sim A(t_p)\theta_p/\theta_E$ , where  $A(t_p)$  is the magnification at the time  $t_p$  of the perturbation, and  $\theta_p \equiv q^{1/2}\theta_E$  is the Einstein ring radius of the planet. The detection probabilities (given the existence of a planet) range from tens of percent for Jovian planets to a few percent for Earth-mass planets (Gould & Loeb 1992; Bennett & Rhie 1996). Since the planet must be located near one of the two primary images in order to yield a detectable deviation, and these images are always located near the Einstein ring radius when the source is significantly magnified, the sensitivity of the microlensing method peaks for planet-star separations of  $\sim \theta_E d_l$ . Detecting planets via the main channel requires substantial commitment of resources because the unpredictable nature of the perturbation requires dense, continuous sampling, and furthermore the detection probability per event is relatively low so many events must be monitored.

The other channel by which microlensing can detect planets is in high magnification events (Griest & Safizadeh 1998). In addition to perturbing images that happen to pass nearby, planets will also distort the perfect circular symmetry of the Einstein ring. Near the peak of high-magnification events, as the lens passes very close to the observer-source line of sight (i.e. when  $u \ll 1$ ), the two primary images are highly elongated and sweep along the Einstein ring, thus probing this distortion. For very high-magnification events ( $A \gtrsim 100$ ), these images probe nearly the entire Einstein ring radius and so are sensitive to all planets with separations near  $\theta_E d_l$ , regardless of their orientation with respect to the source trajectory. Thus high-magnification events can have nearly 100% sensitivity to planets near the Einstein ring radius, and are very sensitive to low-mass planets (Griest & Safizadeh 1998). However, these events are rare: a fraction  $\sim 1/A$  of events have maximum magnification  $\gtrsim A$ . However, these events can often be predicted several hours to several days ahead of peak, and furthermore the times of high sensitivity to planets are within a full-width half-maximum of the event peak, or roughly a day for typical high-magnification events (Rattenbury et al. 2002). Thus scarce observing resources can be concentrated on these few events and only during the times of maximum sensitivity. Because the source stars are highly magnified, it is also possible to use more common, smaller-aperture telescopes.

## 2.1. Peculiarities and Features of the Microlensing Method

The unique way in which microlensing finds planets leads to some useful features, as well as some (mostly surmountable) drawbacks. Most of the features of the microlensing method can be understood simply as a result of the fact that planet detection relies on the direct perturbation of images by the gravitational field of the planet, rather than on light from the planet, or the indirect effect of

the planet on the parent star.

- **Peak Sensitivity Beyond the Snow Line.** The peak sensitivity of microlensing is for planet-star separations of  $\sim \theta_E d_l$ , which corresponds to equilibrium temperatures of

$$T_{\text{eq}} = 278 \text{ K} \left( \frac{L}{L_\odot} \right)^{1/4} \left( \frac{\theta_E d_l}{\text{AU}} \right)^{-1/2} \sim 70 \text{ K} \left( \frac{M}{0.5 M_\odot} \right), \quad (1)$$

where I have assumed  $L/L_\odot = (M/M_\odot)^5$ ,  $d_l = 4 \text{ kpc}$ , and  $d_s = 8 \text{ kpc}$ . Microlensing is most sensitive to planets in the regions beyond the ‘snow line,’ the point in the protoplanetary disk exterior to which the temperature is less than the condensation temperature of water (Lecar et al. 2006; Kennedy & Kenyon 2007). Giant planets are thought to form in the region immediately beyond the snow line, where the surface density of solids is highest.

Microlensing is not sensitive to planets with separations much smaller than the Einstein ring radius, as these can only perturb highly demagnified images. Thus microlensing is much less sensitive to planets in the habitable zones of their parent stars (Park et al. 2006).

- **Sensitivity to Low-mass Planets** The amplitudes of the perturbations caused by planets are typically large,  $\gtrsim 10\%$ . Furthermore, although the durations of the perturbations get shorter with planet mass (as  $\sqrt{m_p}$ ) and the probability of detection decreases (also as  $\sqrt{m_p}$ ), the amplitude of the perturbations are independent of the planet mass. This holds until the ‘zone of influence’ of the planet, which has a size  $\sim \theta_p$ , is smaller than the angular size of the source  $\theta_*$ . When this happens, the perturbation is ‘smoothed’ over the source size. For typical parameters,  $\theta_p \sim \mu\text{as}(m_p/M_\oplus)^{1/2}$ , and for a turn-off star in the bulge  $\theta_* \sim \mu\text{as}$ , so this ‘finite source’ suppression begins to become important for planets with the mass of the Earth, but does not completely suppress the perturbations until masses below that of Mars for main-sequence sources (Bennett & Rhie 1996).

- **Sensitivity to Long-Period and Free-Floating Planets.** Since microlensing can ‘instantaneously’ detect planets without waiting for a full orbital period, it is sensitive to planets with very long periods. Although the probability of detecting a planet decreases for planets with separations larger than the Einstein ring radius because the magnifications of the images decline, it does not drop to zero. Indeed since microlensing is directly sensitive to the planet mass, planets can be detected even without a primary microlensing event. Even free-floating planets that are not bound to any host star are detectable in this way (Han et al. 2005). Microlensing is the only method that can detect old, free-floating planets. A significant population of such planets is a generic prediction of most planet formation models, particular those that invoke strong dynamical interactions to explain the observed eccentricity distribution of planets (Goldreich et al. 2004; Juric & Tremaine 2007; Ford & Rasio 2007).

- **Sensitivity to Planets Throughout the Galaxy.** Because microlensing does not rely on light from the planet or host star, planets can be detecting orbiting stars with distances of several kiloparsecs. The host stars probed by microlensing are simply representative of the population of massive objects along the line of sight to the bulge sources, weighted by the lensing probability. The lensing probability peaks for lens distances about halfway to the sources

in the Galactic bulge, but remains substantial for lens distances in the range  $d_l \sim 1 - 8$  kpc. Specialized surveys may be sensitive to planets with  $d_l \lesssim 1$  kpc (Gaudi et al. 2007), as well as planets in M31 (Covone et al. 2000).

• **Sensitivity to Planets Orbiting a Wide Range of Host Stars.** The sensitivity of microlensing is weakly dependent on the host star mass, and has essentially no dependence on the host star luminosity. Thus microlensing is about equally sensitive to planets orbiting stars all along the main sequence, from brown dwarfs to the main-sequence turn-off, as well as planets orbiting white dwarfs, neutron stars, and black holes (Gould 2000a).

• **Sensitivity to Multiple-Planet Systems.** For the main detection channel, multiple planets in the same system can be detected only if both planets happen to have projected positions sufficiently close to the paths of the two images created by the primary lens. The probability of this is simply the product of the individual probabilities, or  $\mathcal{O}(1\%)$  (Han & Park 2002). In high-magnification events, however, individual planets are detected with near-unity probability regardless of the orientation of the planet with respect to the source trajectory. This immediately implies all planets sufficiently close to the Einstein ring radius will be revealed in such events (Gaudi et al. 1998). This, along with the fact that high-magnification events are potentially sensitive to very low-mass planets, makes such events excellent probes of planetary systems.

## 2.2. What Can We Learn About the Planets and Host Stars?

It has often been stated that the ability of microlensing to provide detailed information about individual systems is very limited. This perception comes from the fact that (1) the host stars are typically distant and faint, making follow-up work is difficult, (2) in the overwhelming majority of microlensing events, the only parameter that can be constrained which contains any information about the primary lens is the event timescale  $t_E$ , which is a degenerate combination of mass, distance, and transverse velocity of the lens, (3) microlensing detections routinely provide only the mass ratio of the planet and host star (Gaudi & Gould 1997), and so the mass of the planet is typically not known without a constraint on the primary mass, and furthermore (4) the only constraint on the planet orbit is  $b_\perp$ , the instantaneous angular separation between the planet and host star at the time of the event in units of  $\theta_E$  (Gaudi & Gould 1997). Since  $\theta_E$ , the inclination, phase, and ellipticity of the orbit are all unknown,  $b_\perp$  provides very little information about the orbit. In the cases when only  $t_E$ ,  $q$ , and  $b_\perp$  can be measured, constraints on the mass and distance to the lens, and mass and semimajor axis of the planet, must rely on a Bayesian analysis which incorporates priors on the distribution of microlens masses, distances and velocities (e.g., Dominik 2006; Dong et al. 2006).

Experience has shown that, in reality, much more information can typically be gleaned from a combination of a detailed analysis of the light curve and follow-up, high-resolution imaging. Several additional pieces of information are potentially available.

• **Finite Source Effects:** For the majority of planets detected via microlensing, the ‘smoothing’ effects of the finite source size are detectable during sharp features in the light curve caused by the planet. The magnitude of this effect is set by  $\rho_* \equiv \theta_*/\theta_E$ , and since  $\theta_*$  can be inferred from the color and magnitude of

the source, this allows a measurement of  $\theta_E$  (Gould 1994).

•**Micro lens Parallax:** In at least three of the planetary microlensing events, it has also been possible to measure the deviations in the microlensing light curve caused by the fact that the Earth is accelerating (Gould 1992). These deviations are generally only significant for events with timescales that are a significant fraction of a year, and so long as compared to the median timescale of  $\sim 20$  days. However, due to selection effects, the majority of planetary events have been long timescale. This ‘microlens parallax’ allows one to constrain  $\tilde{r}_E$ , the Einstein ring radius projected onto the observer plane.

•**Light from the Lens:** Although the lenses are expected to be distant and low-mass, and so faint, it is nevertheless possible to detect some main-sequence lenses during and/or after the event and measure their flux to reasonable precision (often in several different filters). This allows for a photometric estimate of the lens mass and distance (Bennett et al. 2007a).

•**Proper Motion of the Lens:** For microlensing events toward the Galactic bulge, the relative lens-source proper motions are  $\mu_{\text{rel}} \sim 5 - 10$  mas/yr. Thus, after  $\sim 5 - 10$  years, the lens and source will be displaced by  $\sim 0.05$  arcseconds. For luminous lenses, and using space telescope or adaptive optics imaging, it is possible measure the relative lens-source proper motion, either by measuring the elongation of the PSF or by measuring the difference in the centroid in several filters if the lens and source have significantly different colors (Bennett et al. 2007a). The proper motion can be combined with the timescale to give the Einstein ring radius,  $\theta_E = \mu_{\text{rel}} t_E$ .

•**Orbital Motion of the Planet:** In at least two cases, the orbital motion of the planet during the microlensing event has been detected. The effects of orbital motion generally allow the measurement of the two components of the projected velocity of the planet relative to the primary star. If an external measurement of the mass of the lens is available, and under the assumption of a circular orbit, these two components of the projected velocity completely specify the full orbit of the planet (including inclination), up to a two-fold degeneracy (Dong et al. 2008). In some unusual cases, higher-order effects of orbital motion can be used to break this degeneracy and even constrain the ellipticity of the orbit.

In many cases, several of these pieces of information can be measured in the same event, often providing complete or even redundant measurements of the mass, distance, and transverse velocity of the event. For example, a measurement of  $\theta_E$  from finite source effects, when combined with a measurement of  $r_E$  from microlens parallax, yields the lens mass  $M = (c^2/4G)\tilde{r}_E\theta_E$ , distance  $d_l^{-1} = \theta_E/\tilde{r}_E + d_s^{-1}$ , and transverse velocity (Gould 2000b).

### 3. How Microlensing Planet Searches Work (or Don’t) in Practice

The microlensing event rate toward the Galactic bulge is  $\mathcal{O}(10^{-6})$  events per star per year. In a typical field toward the Galactic bulge, the surface density of stars is  $\sim 10^7$  stars per  $\text{deg}^2$  to  $I \sim 20$ . Thus to detect  $\sim 100$  events per year,  $\sim 10 \text{ deg}^2$  of the Bulge must be monitored. Current large-format CCD cameras typically have fields of view of  $\sim 0.25 \text{ deg}^2$ , and thus  $\sim 40$  pointings are required and so fields can only be monitored once or twice per night. While this cadence

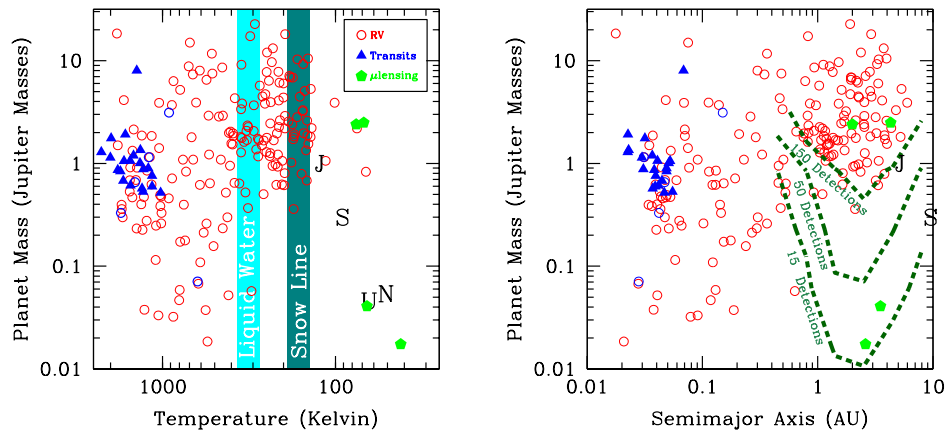


Figure 1. **Left** Extrasolar planets detected via transits (triangles), RV (circles), and microlensing (hexagons), as a function of their mass and equilibrium temperature. Blue circles are planets found via RV that were subsequently found to be transiting. Also shown are the approximate locations of the habitable zone (e.g., Kasting et al. 1993) and the snow line (e.g., Kennedy & Kenyon 2007; Lecar et al. 2006). **Right** Same as the right panel, but versus semimajor axis. The contours show the anticipated number of detections per year from a next-generation microlensing survey, assuming all stars have planet with the given mass or semimajor axis.

is sufficient to detect the primary microlensing events, it is insufficient to detect and characterize planetary perturbations, which last a few days or less.

Thus microlensing planet searches currently operate using a two-stage process. The Optical Gravitational Lens Experiment (OGLE, Udalski et al. 2002) and the Microlensing Observations in Astrophysics (MOA, Abe et al. 2004) collaborations monitor several tens of square degrees of the Galactic bulge, reducing their data real-time in order to alert microlensing event in progress. A subset of these alerted events are then monitored by two follow-up collaborations, a joint venture of the Probing Lensing Anomalies NETwork (PLANET, Albrow et al. 1998) and RoboNet (Burgdorf et al. 2007) collaborations, and the Microlensing Follow Up Network ( $\mu$ FUN, Yoo et al. 2004). Since only individual events are monitored, these teams can achieve the sampling and photometric accuracy necessary to detect planetary perturbations. In fact, the line between the ‘alert’ and ‘follow-up’ collaborations is somewhat blurry, both because the MOA and OGLE collaborations monitor some fields with sufficient cadence to detect a subset of the longest planetary perturbations, and because there is a high level of communication between the collaborations, such that the observing strategies are often altered real time based on available information about ongoing events.

The PLANET/RoboNET collaboration has substantial access to 0.6-1.5m telescopes located in Chile, South Africa, Perth, and Tasmania. With these resources, they are able to monitor dozens of events per season, and so are able to search for planets via the main channel. This tactic led to the detection of the first cool rocky/icy exoplanet OGLE-2005-BLG-390Lb (Beaulieu et al. 2006).

The  $\mu$ FUN collaboration takes a different approach, motivated by its more shoe-string, slipshod nature. They use a single 1m telescope in Chile to monitor promising alerted events in order try to identify high-magnification events substantially before peak. Since high-magnification events are relatively rare ( $\sim 5$  per year), for the majority of the time, nothing happens. However, when a likely high-magnification event is imminent, they notify the other telescopes in the collaboration, and then instruct them to ‘go all out’ during the high-magnification peak. Thus  $\mu$ FUN adopts what can best be described as a “wait... wait... wait... PANIC” approach to searching for planets. Since  $\mu$ FUN focuses on high-magnification events, which often reach peak magnitudes of  $I \lesssim 15$ , their targets are usually within reach of the relatively small-aperture (0.3-0.4m) telescopes commonly owned by enthusiastic amateur astronomers. Indeed, over half of the members of the  $\mu$ FUN collaboration are amateurs. These amateurs often contribute crucial data: in the majority of the  $\mu$ FUN planet detections, data from amateur telescopes were essential for the proper interpretation of the events. In the words of one amateur member of  $\mu$ FUN:

*“It just shows that you can be a mother, you can work full-time, and you can still go out there and find planets.”* -Jenny McCormick, Farm Cove Observatory

The real-time identification of high-magnification events is a difficult business, and is often prone to human error, as well as human inspiration. For example, in the case of microlensing event OGLE-2004-BLG-343, an internal alert was ignored and as a result the peak of this magnification  $\sim 3000$  event was missed. Subsequent analysis demonstrated that had the peak been intensely monitored, the event would have provided significant sensitivity to Earth-mass planets (Dong et al. 2006). On the other hand, in the case of the magnification  $\sim 800$  event OGLE-2005-BLG-169, the specific instructions of a senior scientist to gather a few data points were explicitly ignored by an insubordinate graduate student, and instead said graduate student obtained over 1000 points over the peak, resulting in the detection of a Neptune-mass planet (Gould et al. 2006).

#### 4. What We’ve Found: Results to Date

The microlensing method was first proposed in 1991, and microlensing planet searches began in earnest in 1995. From 1995-2001, only  $\sim 50 - 100$  events were alerted per year. As a result, there were few high magnification events each year, and only a handful of events ongoing at any time. The follow-up collaborations were therefore not able to ‘pick and choose’ the best events for follow-up. Indeed, no convincing planet detections were made during this period, although interesting upper limits were placed on the frequency of Jovian planets based on detailed analyses of the sensitivities of the various searches (Gaudi et al. 2002; Snodgrass et al. 2004). Perhaps the most important result of this period, however, was the development of both the theory and practice of the microlensing method, which resulted in its transformation from a theoretical abstraction to a viable, practical method of searching for planets.

In 2001, the OGLE collaboration upgraded to a new camera with a 16 times larger field of view and so were able to monitor a larger area of the bulge with



a higher cadence. As a result, in 2002 OGLE began alerting nearly an order of magnitude more events per year than previous to the upgrade. These improvements in the alert rate and cadence, combined with improved cooperation and coordination between the survey and follow-up collaborations, led to the first discovery of an extrasolar planet with microlensing in 2003. MOA upgraded to a 1.8m telescope and 2 deg<sup>2</sup> camera in 2004, and together OGLE and MOA collaborations now alert  $\sim 850$  events per year.

To date, there are four published planet detections with microlensing. The masses, separations, and equilibrium temperatures of these planets are shown in Figure 1. The first two planets found by microlensing, OGLE-2003-BLG-235/MOA-2003-BLG-53Lb (Bond et al. 2004), and OGLE-2005-BLG-071Lb (Udalski et al. 2005), are Jovian-mass objects with separations of  $\sim 2-4$  AU. While the masses and separations of these planets are similar to many of the planets discovered via radial velocity surveys, their host stars are generally less massive and so the planets have substantially lower equilibrium temperatures of  $\sim 70$  K, similar to Saturn and Uranus.

The third and fourth planets discovered by microlensing are significantly lower mass, and indeed inhabit a region of parameter space that was previously unexplored by any method. OGLE-2005-BLG-390Lb is a very low-mass planet with a planet/star mass ratio of only  $\sim 8 \times 10^{-5}$  (Beaulieu et al. 2006). A Bayesian analysis combined with a measurement of  $\theta_E$  from finite source effects indicates that the planet likely orbits a low-mass M dwarf with  $M = 0.22^{+0.21}_{-0.11} M_\odot$ , and thus has a mass of only  $5.5^{+5.5}_{-2.7} M_\oplus$ . Its separation is  $2.6^{+1.5}_{-0.6}$  AU, and so has an extremely cool equilibrium temperature of  $\sim 50$  K. OGLE-2005-BLG-169Lb is another low-mass planet with a mass ratio of  $8 \times 10^{-5}$  (Gould et al. 2006), essentially identical to that of OGLE-2005-BLG-390Lb. A Bayesian analysis indicates a primary mass of  $0.52^{+0.19}_{-0.22} M_\odot$ , and so a planet of mass  $\sim 14^{+5}_{-6} M_\oplus$ , a separation of  $3.3^{+1.9}_{-0.9}$  AU, and so an equilibrium temperature of  $\sim 70$  K. In terms of its mass and equilibrium temperature, OGLE-2005-BLG-169Lb is very similar to Uranus. OGLE-2005-BLG-169Lb was discovered in a high-magnification  $A \sim 800$  event; as argued above, such events have significant sensitivity to multiple planets. There is no indication of any additional planetary perturbations in this event, which excludes Jupiter-mass planets with separations between 0.5-15 AU, and Saturn-mass planets with separations between 0.8-9.5 AU. Thus it appears that this planetary system is dominated by the Neptune-mass companion.

The microlensing detection sensitivity declines with planet mass as  $\sqrt{m_P}$ , and thus the presence of two low-mass planets in a sample of four detections argues that the frequency of cool “Neptunes” ( $5-15 M_\oplus$ ) is substantially higher than that of cool Jovian-class planets. A quantitative analysis that accounts for the detection sensitivities and Poisson statistics shows that, at 90% confidence,  $38^{+31}_{-22}\%$  of stars host cool Neptunes with separations in the range 1.6 – 4.3 AU (Gould et al. 2006). Thus, these planets are common, which is ostensibly a confirmation of the core accretion model of planet formation, which predicts that there should exist many more ‘failed Jupiters’ than bona-fide Jovian-mass planets at such separations, particularly around low-mass primaries.

In all of the planet detections, it has been possible to obtain additional information to improve the constraints on the properties of the primaries and

planets. In all four cases, finite source effects have been detectable and so it has been possible to measure  $\theta_E$ . For OGLE-2003-BLG-235/MOA-2003-BLG-53Lb, follow-up imaging with the *Hubble Space Telescope* (*HST*) yielded a detection of light from the lens, which constrains the mass of the primary to  $\sim 15\%$ ,  $M = 0.63^{+0.07}_{-0.09} M_\odot$  (Bennett et al. 2006). In the case of OGLE-2005-BLG-071Lb, *HST* photometry, when combined with information on finite source effects and microlens parallax from the light curve, leads to the conclusion that the primary lens is a mid-M dwarf with a mass of  $M = 0.35 \pm 0.05 M_\odot$  and a distance of  $d_l = 3.1 \pm 0.4$  kpc (Dong et al. 2008). Furthermore, the velocity of the primary is constrained to be  $v_{\text{LSR}} = 110 \pm 25$  km s $^{-1}$  and there is evidence at the  $\sim 2\sigma$  level that the host has a subsolar metallicity. Thus, OGLE-2005-BLG-071Lb may be a massive Jovian planet orbiting a metal-poor, thick-disk, mid M-dwarf. The existence of such a planet may pose a challenge for core-accretion models of planet formation (e.g., Laughlin et al. 2004; Ida & Lin 2004, 2005). Although this result should be taken as tentative, and must be confirmed with additional measurements, it nevertheless demonstrates that it is possible to obtain fairly detailed information on individual planetary systems detected via microlensing.

## 5. Where We Are Going: the Short and Long-Term Future

With the recent MOA upgrade, the rate of planet detections has increased substantially. From 2003-2006, six planets were detected (four have been published). From the 2007 bulge season alone, there are four fairly secure planetary events. This rate can be expected to increase modestly as analysis techniques improve, and so the next several years should bring of order a dozen planet detections.

The new MOA setup points the way toward the next generation of microlensing planet searches, which will operate in a very different mode than the current alert/follow-up model. With a sufficiently large field-of-view (FOV) of 2-4 deg $^2$ , it becomes possible to monitor tens of millions of stars every 10–20 minutes, and so discover thousands of microlensing events per year. Furthermore, these would be simultaneously monitored to search for planetary perturbations. In order to obtain round-the-clock coverage and so catch all of the perturbations, several such telescopes would be needed, located on 3-4 continents roughly evenly spread in longitude. Detailed simulations of such a next-generation microlensing survey have been performed by several groups. These simulations include models for the Galactic population of lenses and sources that match all constraints, and account for real-world effects such as weather, variable seeing, moon and sky background, and crowded fields. They reach similar conclusions. Such a survey would increase the planet detection rate at fixed mass by at least an order of magnitude over current surveys. Figure 2 shows the predictions of these simulations for the detection rate of planets of various masses and separations. In particular, if Earth-mass planets with semimajor axes of several AU are common around main-sequence stars, a next generation microlensing survey should detect several such planets per year. This survey would also be sensitive to free-floating planets, and would detect them at a rate of hundreds per year if every star has ejected Jupiter-mass planet (Gould et al. 2007).

In fact, a next-generation microlensing survey appears to be forming spontaneously. The MOA telescope already represents one leg of such a survey. The

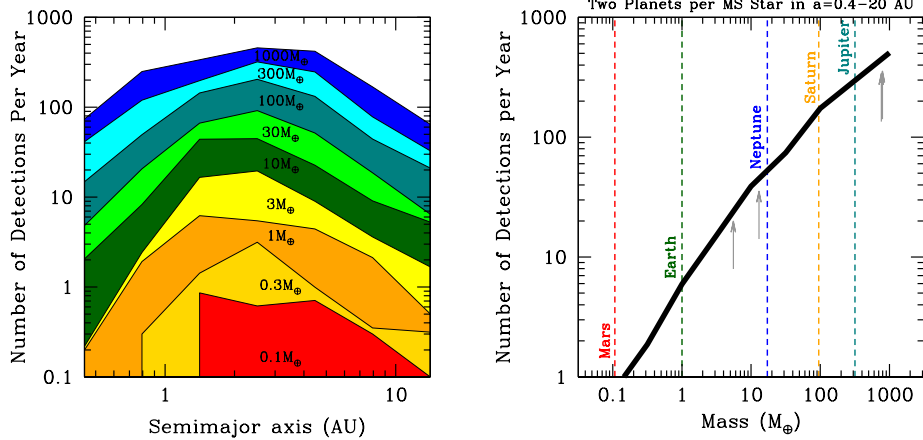


Figure 2. Expectations from a next-generation ground-based microlensing survey. These results represent the average of two independent simulations which include very different input assumptions but differ in their predictions by only  $\sim 0.3$  dex. **Left** Number of planets detected per year assuming every main-sequence (MS) star has a planet of a given mass and semi-major axis. **Right** Same as left panel, but assuming every MS has two planets distributed uniformly in  $\log(a)$  between 0.4–20 AU. The arrows indicate the masses of the four microlensing exoplanet detections.

OGLE team has been funded to upgrade to a  $1.7 \text{ deg}^2$  camera, which would represent the second leg. Astronomers from Korea, Germany, and China are considering initiatives to secure funding to build 1–2m class telescopes with wide FOV cameras in southern Africa or Antarctica. If these plans are realized, a next-generation survey would effectively be in place that could realize a significant fraction of the yields shown in Figure 2.

Ultimately, however, the true potential of microlensing cannot be realized from the ground. Weather, seeing, crowded fields, and systematic errors all conspire to make the detection of planets with mass less than Earth effectively impossible from the ground. A space-based microlensing survey offers several advantages: the main-sequence bulge sources needed to detect sub-Earth mass planets are resolved from space, the events can be monitored continuously, and it is possible to observe the moderately reddened source stars in the near infrared to improve the photon collection rate. Furthermore, the high spatial resolution afforded by space allows unambiguous identification of light from the primary (lens) stars and so measurements of the primary and planet masses.

The expectations from a Discovery-class space-based microlensing survey are impressive. Such a survey would be sensitive to all planets with mass  $\gtrsim 0.1 M_{\oplus}$  and separations  $a \gtrsim 0.5 \text{ AU}$ , including free-floating planets. This range includes analogs to all the solar system planets except Mercury. If every main-sequence star has an Earth-mass planet in the range 1–2.5 AU, the survey would detect  $\sim 500$  such planets within its mission lifetime. When combined with complementary surveys such as *Kepler*, such a survey would yield an accurate and complete census of both bound and free-floating planets with masses greater

than that of Mars orbiting stars with masses less than that of the Sun. Such a census would likely provide the ultimate test of planet formation theories.

**Acknowledgments.** I would like to acknowledge the many people who have contributed to the work described in this short review, and in particular Andy Gould, David Bennett, Subo Dong, and my fellow members of the  $\mu$ FUN collaboration. I would like to thank Fred Rasio, Alex Wolszczan, and the other organizers for the putting together an amazing conference.

## References

- Abe, F., et al. 2004, *Science*, 305, 1264  
 Albrow, M., et al. 1998, *ApJ*, 509, 687  
 Beaulieu, J.-P., et al. 2006, *Nat*, 439, 437  
 Bennett, D. P., & Rhie, S. H. 1996, *ApJ*, 472, 660  
 Bennett, D., Anderson, J., Bond, I., Udalski, A., & Gould, A. 2006, *ApJ*, 647, L171  
 Bennett, D. P., Anderson, J., & Gaudi, B. S. 2007a, *ApJ*, 680, 781  
 Bennett, D. P., et al. 2007b, *ExoPTF White Paper* (arXiv:0704.0454)  
 Burgdorf, M. J., et al. 2007, *P&SS*, 55, 582  
 Bond, I. A., et al. 2004, *ApJ*, 606, L155  
 Covone, G., de Ritis, R., Dominik, M., & Marino, A. A. 2000, *A&A*, 357, 816  
 Dominik, M. 2006, *MNRAS*, 367, 669  
 Dong, S., et al. 2006, *ApJ*, 642, 842  
 Dong, S., et al. 2008, in preparation  
 Ford, E. B., & Rasio, F. A. 2007, *ApJ*, submitted (astro-ph/0703163)  
 Gaudi, B. S., & Gould, A. 1997, *ApJ*, 486, 85  
 Gaudi, B. S., Naber, R. M., & Sackett, P. D. 1998, *ApJ*, 502, L33  
 Gaudi, B. S., et al. 2002, *ApJ*, 566, 463  
 Gaudi, B. S., et al. 2007, *ApJ*, submitted (astro-ph/0703125)  
 Goldreich, P., Lithwick, Y., & Sari, R. 2004, *ApJ*, 614, 497  
 Gould, A. 1992, *ApJ*, 392, 442  
 Gould, A., & Loeb, A. 1992, *ApJ*, 396, 104  
 Gould, A. 1994, *ApJ*, 421, L71  
 Gould, A. 2000a, *ApJ*, 535, 928  
 Gould, A. 2000b, *ApJ*, 542, 785  
 Gould, A., et al. 2006, *ApJ*, 644, L37  
 Gould, A., Gaudi, B. S., & Bennett, D. P. 2007, *ExoPTF White Paper* (arXiv:0704.0767)  
 Griest, K., & Safizadeh, N. 1998, *ApJ*, 500, 37  
 Han, C., & Park, M.-G. 2002, *Journal of Korean Astronomical Society*, 35, 35  
 Han, C., Gaudi, B. S., An, J. H., & Gould, A. 2005, *ApJ*, 618, 962  
 Ida, S., & Lin, D. N. C. 2004, *ApJ*, 616, 567  
 Ida, S., & Lin, D. N. C. 2005, *ApJ*, 626, 1045  
 Juric, M., & Tremaine, S. 2007, *ApJ*, submitted (astro-ph/0703160)  
 Kasting, J. F., Whitmire, D. P., & Reynolds, R. T. 1993, *Icarus*, 101, 108  
 Kennedy, G. M., & Kenyon, S. J. 2007, *ApJ*, in press (arXiv:0710.1065)  
 Laughlin, G., Bodenheimer, P., & Adams, F. C. 2004, *ApJ*, 612, L73  
 Lecar, M., Podolak, M., Sasselov, D., & Chiang, E. 2006, *ApJ*, 640, 1115  
 Mao, S., & Paczynski, B. 1991, *ApJ*, 374, L37  
 Park, B.-G., Jeon, Y.-B., Lee, C.-U., & Han, C. 2006, *ApJ*, 643, 1233  
 Rattenbury, N. J., Bond, I. A., Skuljan, J., & Yock, P. C. M. 2002, *MNRAS*, 335, 159  
 Snodgrass, C., Horne, K., & Tsapras, Y. 2004, *MNRAS*, 351, 967  
 Udalski, A., et al. 2002, *Acta Astronomica*, 52, 1  
 Udalski, A., et al. 2005, *ApJ*, 628, L109  
 Yoo, J., et al. 2004, *ApJ*, 603, 139